Membrane Switch Hypothesis. 1. Cell Density Influences Lateral Domain Structure of Tumor Cell Membranes

Tilen Koklič,*,† Mateja Pirš,‡ Reiner Zeisig,§ Zrinka Abramović,† and Marjeta Šentjurc†

EPR Center, "Jožef Stefan" Institute, Jamova 39, 1001 Ljubljana, Slovenia, Department of Infectious Diseases, University Clinical Center Ljubljana, Japljeva 2, Ljubljana, Slovenia, and Experimental Pharmacology Department, Max-Delbrück-Centre for Molecular Medicine, Robert-Rössle Strasse 10, 13122 Berlin-Buch, Germany

Received May 5, 2005

The domain structure of human cancer cells membranes was investigated by electron paramagnetic resonance (EPR) in different phases of cell growth, and the results were compared to those obtained for nonmalignant cells. On the basis of computer simulation of the EPR spectra using a newly developed GHOST condensation routine it was suggested that plasma membranes of cancer cells have less lateral lipid domain types at confluent conditions than in the exponential growing phase, while in nonmalignant cells the domain structure does not change significantly during cell growth. In accordance to our experimental data we propose a membrane switch hypothesis: disappearance of certain membrane domain types might act as a switch promoting the clustering of membrane constituents into the active units in a common lipid membrane domain and thus influencing the physiology of cells.

INTRODUCTION

Implication of membrane fluidity alteration in various diseases includes diabetes, obesity, hypertension, cancer, neurological, and heart diseases.[1] Research done by other groups[2−4] and observations of our group[5,6] showed that in malignant cells membrane fluidity in general is higher as in normal cells. But it is still unclear which specific processes during tumor growth are affected by this membrane property. Proliferative activity of a certain cell type generally increases with increased membrane fluidity.[2] While normal cells possess defined membrane fluidity at their stationery state, membrane fluidity of proliferative cells can be affected by the cell density, the cell cycle, and the lipid metabolism as well as by the external tissue or fluid.[7]

In a recent model of cell membranes the concept of fluidity in the original Singer−Nicolson[8] model is interpreted as permissiveness to continuous dynamic restructuring of molecular and higher-level clusters according to the needs of the cell and as evoked by the environment.[9] From the analysis of the diffusion of transmembrane proteins and lipids, compartments seem to be a general structure of the cell membrane, with the compartment size ranging from several ten to several hundred nanometers.[10,11] By conventional EPR different modes of rotational movement of an ensemble of molecules can be observed, which could correspond to different types of coexisting domains with different motional characteristics inside the membrane compartments. The membrane compartments cannot be resolved by conventional EPR, but some motional modes could correspond to the restricted motion of lipids nearby the immobilized transmembrane proteins. Different types of membrane domains with different fluidity characteristics can alter with time, cell growth, and with different physiological conditions.

In this work we have studied the changes in the domain structure of the plasma membrane of tumor cells in different phases of cell growth and compare it with that of the plasma membrane of nonmalignant cell lines. In this way we wanted to gain a more detailed insight into a heterogeneous structure of the plasma membrane and its changes during cell growth or with increasing cell density, which could provide us with the understanding of the role of the plasma membrane in the physiological processes of tumor cells.

MATERIALS AND METHODS

Materials. The spin probe 5-doxylpalmitoyl methyl ester (MeFASL(10,3)) was synthesized by S. Pečar (Faculty of Pharmacy, University of Ljubljana, Ljubljana, Slovenia). Media and additives for cell culturing were obtained from Gibco − Invitrogen Corporation (Carlsbad, California). Bio-Rad Protein Assay (Bio-Rad Laboratories, München, Germany) was used to determine the protein content in cells.

Human cancer cell lines MT1, MT3, NCl (all human breast cancer cells, of different sizes and different growing rates) and HeLa (human cervical adenocarcinoma) and nonmalignant cell lines V79 (hamster fibroblasts) and HEK-293 (human embryonic kidney) were used in our experiments.

Cell Culturing. The cell lines were cultured in RPMI-1640 medium (Gibco) and supplemented with 2 μmol/mL of L-glutamine (Gibco), penicillin (100 U/mL), streptomycin (100 μg/mL), and heat-inactivated fetal calf serum (10% FCS, Gibco), at 37 °C, 90% humidity, and 5% CO_2. Cells were passaged at subconfluence by trypsination (0.25% in PBS). For all experiments, $9 \cdot 10^5$ cells were seeded in a 25 cm^2 cell culture flask. In some experiments the medium was

* Corresponding author phone: +386 1 477 34 38; fax: +386 1 477 31 91; e-mail: tilen.koklic@ijs.si.
† EPR Center, "Jožef Stefan" Institute.
‡ University Clinical Center Ljubljana.
§ Max-Delbrück-Centre for Molecular Medicine.

10.1021/ci050186r CCC: $30.25
Published on Web 10/29/2005

changed each day, and in some experiments it was changed on day 3 and day 7. On the day of the measurement cells were washed twice with RPMI-1640 medium and harvested with a rubber policeman, at different times of cell growth.

Their viability was checked by trypan blue exclusion and was about 65% for MT3 cells and about 75 to 80% for V79 and HeLa cells and increased with the time of growth for about 15 to 20% for V79 and MT3, while it remained the same for HeLa cells. In all phases of cell growth they looked unchanged. The number of cells in a specimen was calculated after counting cells using Bürker−Türck's chamber, and the protein content per number of cells was determined spectrophotometrically by Bio-Rad protein assay.[12] The experiments were repeated at least three times, with the cells from different passages.

EPR Measurements. For EPR measurements a 3 mL suspension of $5 \cdot 10^6$ cells was spin labeled with 25 μL 10^{-4} mol/L of lipophilic spin probe MeFASL(10,3) in the following way: a thin film of MeFASL(10,3) was prepared on the wall of a glass tube by rotary evaporation of an ethanol solution of the spin probe. The suspension of cells was then added, and the tube was lightly shaken by hand at room temperature for 10 min. After that the samples were centrifuged, at 120·g for 2 min, and the supernatant was carefully removed. The remaining pellet of cells was transferred into a glass capillary (approximately 1 mm in diameter) for EPR measurements, which were performed on an X-band EPR spectrometer Bruker ESP 300 at room temperature, with microwave frequency 9.59 GHz, power 20 mW, modulation frequency 100 kHz, and amplitude 0.2 mT.

Computer Simulation of EPR Spectra. From the line shape of the EPR spectra information about the overall cell membrane fluidity can be obtained. More precise information about the heterogeneity of the cell membrane and its domain structure can be obtained by computer simulation of the EPR spectra.

To describe the EPR spectra of spin probes, the stochastic Liouville equation is used.[13−15] However, in a membrane system labeled with fatty acid spin probes, measured at room temperatures, local rotational motions are fast with respect to the EPR time scale. Since the basic approach was already discussed elsewhere,[16,17] it is only summarized here. The model takes into account that the spectrum is composed of several spectral components reflecting different modes of restricted rotational motion of spin probe molecules in different environments of the membrane, described with different sets of spectral parameters: order parameter (S), rotational correlation time (τ_c), polarity correction factors of hyperfine (A) and g tensors (p_A and p_g), and broadening constant (W). S is related to time averaged amplitude of rotational motion of the nitroxide group relative to its average direction ($S = 1$ for perfectly oriented molecules and $S = 0$ for isotropic motion of molecules), τ_c describes the rate of motion, polarity correction factors are due to the effect of neighboring electric fields, which influence the electron density distribution of the spin probe, and W arises primarily from unresolved hydrogen super-hyperfine interactions and contributions from other paramagnetic impurities (e.g., oxygen, which is usually present), external magnetic field inhomogeneities, and field modulation effects as well as from spin−spin interaction. It is important to note that the line broadening can differ among the domains due to different partitioning of spin probes and/or oxygen in different regions of the membrane. The simulated EPR spectrum $I(B)$ is composed of N_d ($N_d \leq 5$) spectral components $I_i(B)$

$$I(B) = \sum_{i=1}^{N_d} I_i(B) \cdot d_i \tag{1}$$

where B is the magnetic field, i is the index of a spectral component, and d_i is the relative proportion of the ith spectral component.[18] Therefore

$$\sum_{i=1}^{N_d} d_i = 1 \tag{2}$$

Besides all the other spectral parameters, the relative proportion of a particular spectral component d is determined by finding the best fit to an experimental EPR spectrum. It describes the relative amount of the spin probes with a particular motional mode and depends on the distribution of the spin probe between the domain types as well as on the distribution and position of the spin probe within the domain. If we suppose that the spin probe is equally distributed between the domains, d describes the relative area of the cell membrane, which is occupied with the domains with similar motional characteristics (domain types). It should be stressed that the lateral motion of the spin probe is slow on the time scale of EPR spectra.[19,20] Therefore an EPR spectrum describes only the properties of the nearest surrounding of a spin probe, which is in the range of several 10^{-2} nm. Different modes of rotational movement of an ensemble of molecules can be observed by conventional EPR, which could correspond to different types of coexisting domains with different motional characteristics inside the membrane compartments. The computer simulation procedure is implemented in the software package EPRSIM (http://www.ijs.si/ijs/dept/EPR/).

GHOST Optimization Procedure. To obtain the best fit of calculated to experimental spectra a deterministic and robust optimization method like Simplex Downhill can be applied. It provides good results only if starting points are close to the solutions.[17] This inherently leads to the convergence into a local rather than in a global minimum. To eliminate these problems the stochastic and population-based genetic algorithm is used. This requires no special starting points and no user intervention. It is good at finding promising regions in a complex search space. When combined with Simplex Downhill and knowledge-based operators into an evolutionary optimization method (HEO)[21] it is also capable of fine-tuning.

To get a reasonable characterization one still has to define the number of spectral components before applying the optimization procedure. To resolve this problem multirun HEO optimization is used together with a newly developed GHOST condensation procedure. According to this method 200 independent HEO simulation runs for each EPR spectrum were applied, taking into account 4 different motional modes of a spin probe (23 spectral parameters), which is around the resolution limit of EPR nitroxide experiments. From these runs only the set of parameters, which correspond to the best fits were used. All the best fit

sets of parameters obtained by 200 optimizations were evaluated according to the goodness of the fit (χ^2 filter) and according to the similarity of the parameter values of best fits (density filter). The parameters of the best fits were presented by three two-dimensional cross-section plots using four spectral parameters: order parameter S, rotational correlation time τ_c, line broadening W, and polarity correction factor p_A (S-τ_c, S-W, and S-p_A diagrams, the other two parameters in each diagram are defined by intensity of colors red, green, and blue for τ_c, W, and p_A, respectively).[22] Groups of solutions, which represent the motional modes of spin probes in a particular surrounding and which could correspond to different types of membrane domains, can be resolved either graphically on GHOST diagrams or numerically within GHOST condensation. Even if the number of different motional modes is more than four, some information about the molecular arrangement in the membrane can be obtained.[18,22] From these plots information about the membrane domain types, dynamics of motion, and ordering within the domain types as well as about the polarity of spin probe surrounding can be obtained. Therefore the changes in the domain types due to the interaction of membrane with biologically active compounds, due to the temperature changes or due to inclusion of other molecules into the membrane, can be studied.

RESULTS

Plasma Membrane Fluidity. Plasma membrane fluidity is a membrane characteristic, which can be described with an average ordering and dynamics of membrane lipids and is in opposite relation to membrane microviscosity. In EPR experiments it is described with order parameter S and a rotational rate of lipid chain motion.[2] Average membrane fluidity can be estimated directly from the EPR spectra, while for a better description of motional characteristics in different membrane regions computer simulation of the EPR spectra is necessary.

Figure 1 shows the EPR spectra of the spin probe (MeFASL(10,3)) in malignant (MT1 and HeLa) and in nonmalignant (V79) cells after different times of growth. The spin probe is distributed mainly in cell plasma membranes. Oxy−redoxy systems in cell organelles and in cytoplasm reduce the spin probes to hydoxylamines, which are no longer detectable by EPR.[23,24] Therefore only spin probes in the plasma membrane contribute to the EPR signal.

In Figure 1 an arrow indicates the portion of the spectrum, which corresponds to a more restricted motion of the spin probe and reflects the characteristics of ordered and less fluid membrane domains. This portion of the spectrum was decreasing later with the time of malignant cell growth after the initial increase observed in the first few days of cell growth, and the spectrum, characteristic for less restricted motion, typical for more fluid domains, prevails later. This indicates that the overall membrane fluidity of malignant cells was increasing with the time of growth and was the highest on the last day of growth. In nonmalignant cell lines the line shapes of the EPR spectra did not change with the time of growth and resembled that of malignant cells after 3 days of growing.

To obtain a quantitative estimation of plasma membrane fluidity the line shapes of the EPR spectra were calculated by the computer simulation, and the parameters were varied until the best fits with the experimental spectra were obtained. Since the spectra of different experiments were reproducible, the sum of the spectra of the cells taken from different passages, but which were grown for the same time, was taken for computer simulation.

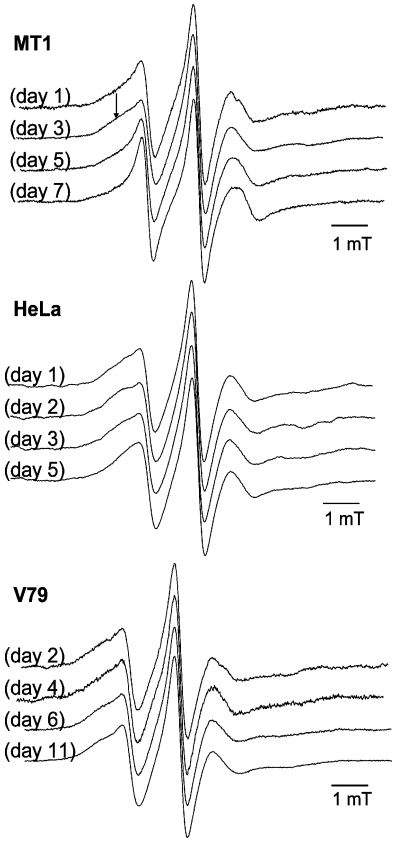

Figure 1. EPR spectra of the lipophilic spin probe methyl ester of 5-doxylpalmitate (MeFASL(10,3)) in the plasma membrane of MT1 breast cancer cells, HeLa cells, and nonmalignant cell line V79 hamster fibroblasts at different times of cell growth.

In the first approximation each EPR spectrum was decomposed to 3 spectral components each representing a mode of spin probe motion in a part of the plasma membrane with defined dynamic properties. The membrane is more fluid when the relative portion of the less ordered domain increases and/or when the order parameter of domains decreases. Since according to the simulation of the experimental spectra the main changes with the time of cell growth are observed in the proportions of membrane domains, and only minor changes were observed in order parameters, we have taken the relative proportion of the most disordered mode of spin probe motion (with the lowest order parameter) as a measure for overall membrane fluidity. In accordance with the line shape of the EPR spectra (Figure 1) the relative proportion of the most disordered mode (the most fluid membrane region) of the spin probe motion decreased until day 3 of cell growth and increased again until the 7th day in malignant breast cancer cells as well as in HeLa cells. A typical example of theses changes is presented in Figure 2 for MT1 cells and is similar to other cancer cell lines investigated in this study.

A pronounced difference in membrane fluidity changes with time of growth was observed when the cells were grown under conditions, where the medium was changed every 3

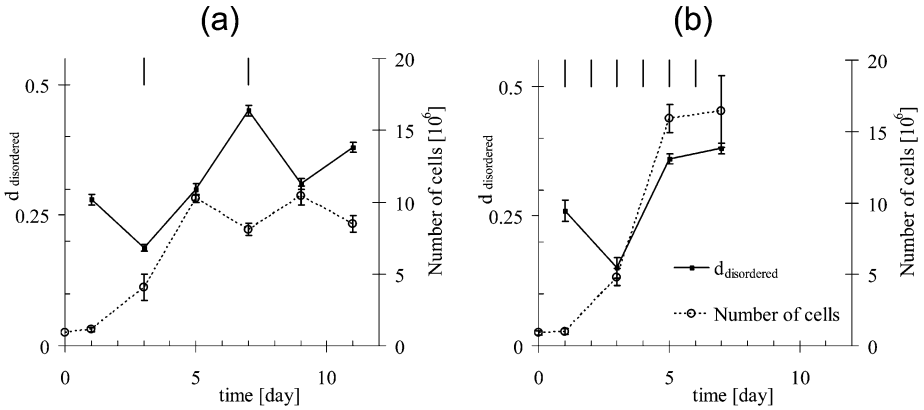

Figure 2. Number of MT1 breast cancer cells at different times of growth (dotted line) and the relative proportion of spin probe in a disordered mode of motion (solid line) ($d_{\text{disordered}}$ − membrane fluidity) in plasma membrane: (a) medium was changed on the third and seventh day (indicated by vertical lines at the top of the graphs) and (b) medium was changed every day.

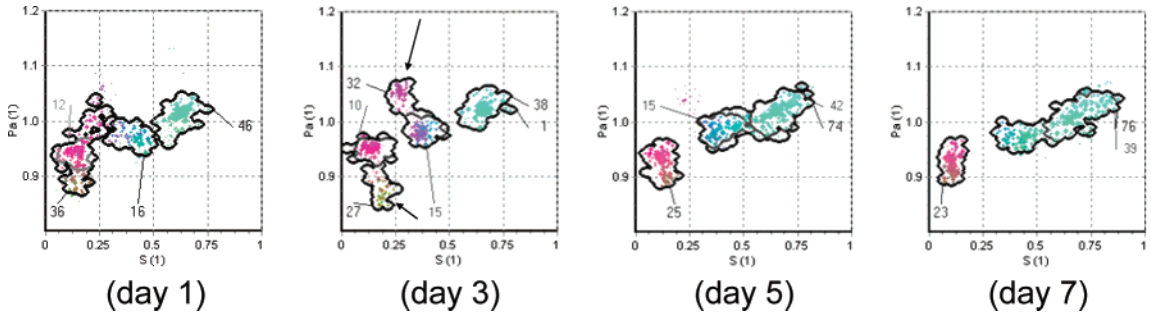

Figure 3. $S-p_A$ (order parameter − polarity correction) GHOST diagrams of EPR spectral parameters of motional modes of spin probes in plasma membrane of MT1 breast cancer cells at different growth times. Arrows in the diagram (day 3) indicate the additional modes of spin probe motion that appear after 3 days of growth.

days (Figure 2a) with respect to the cells grown under conditions where the medium was changed every day (Figure 2b). After 3 days in use the medium becomes depleted of the nutrients which seems to stop the cell growth and increase the portion of disordered domains i.e., increase membrane fluidity. When the medium was changed, the cells started to grow again (day 9 in Figure 2a) and fluidity decreased again. If the medium was regularly changed every day (Figure 2b), the cells grew faster, until they reached the confluent phase (at day 5). This property was also reflected in cell membrane fluidity. After 5 days the cells covered the surface of the flask and the growth of cells slowed; the variations in the number of cells as well as in the proportion of the most disordered domain remained in the range of experimental error. One day after the cells were passaged at subconfluence, i.e., in their lag phase, it seems that they still experienced the similar properties as in the confluent-plateau phase; therefore, their fluidity was higher as on day 3, when they were in the exponential phase of growth. At this time the proportion of the domain types, which are more fluid increased with the time of growth and correspondingly with the density of cells in the flask, until the cells became confluent. Contrary to this, membrane fluidity in nonmalignant cells was much less dependent on the growth phase, on cell density, and on the quality of growing medium. Fluidity of these cells was lower as in malignant cells in accordance to most of the published results.[2−6]

Domain Structure of Plasma Membrane. A better insight into the domain structure of the plasma membrane during the time of cell growth was obtained when the GHOST condensation routine[22] was applied to the EPR spectra. This more detailed handling of data results in GHOST diagrams where several results of computer simulation are joined into groups of solutions, each representing a mode of spin probe motion in a part of the plasma membrane with defined dynamic characteristics of constituent lipids. According to this procedure the number of different modes of motion is not defined before applying computer simulation of an EPR spectrum. All the modes of the spin probe motion in the plasma membrane are found automatically by the GHOST condensation routine. GHOST diagrams for the MT1 cell line at different times of cell growth are presented in Figure 3.

Roughly 3 modes of spin probe motion were generally detected in the plasma membrane of MT1 breast cancer cell lines, except at day 3 of cell growth, when the cells were in the exponential phase (Figure 3). In this situation, two additional modes of spin probe motion were detected (marked with arrows in Figure 3). These two additional modes of spin probe motion began to appear on the GHOST diagram of cells measured after only 1 day of growth (Figure 3); however, they were clearly expressed after 3 days of growth, when the number of cells in a flask was exponentially increasing. One mode of the spin probe motion was characterized with S around 0.3 and p_A in the polar region ($p_A \sim 1.05$) and the other with S around 0.2 in the nonpolar region with p_A around 0.85. These two modes disappeared, when the cells were confluent at day 5 and at day 7 (Figure 3).

The same phenomenon was detected also for the other breast cancer cell lines (Figure 4). Again, two additional modes of spin probe motion were found when the cells were

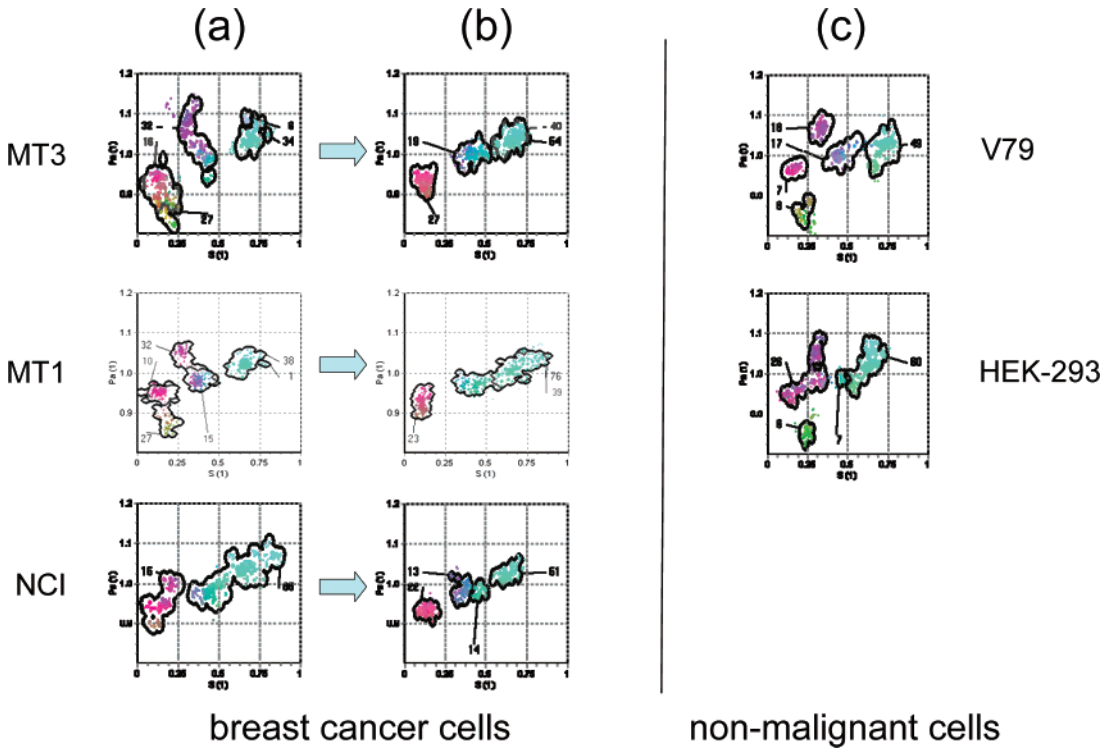

Figure 4. Comparison of the domain structure of the plasma membrane of breast cancer cell lines to nonmalignant cell lines. $S-p_A$ (order parameter − polarity correction) GHOST diagrams of EPR spectral parameters of motional modes of spin probes in the plasma membrane of breast cancer cells: (a) in the exponential phase of growth; (b) in the plateau phase of cell growth; and (c) nonmalignant cells in the exponential phase or plateau phase (the domain structure is approximately the same in exponential and plateau phases).

in the exponential growth phase (Figure 4a), which disappeared when the cells reached confluence. At confluence, only 3 different modes of spin probe motion were detected (Figure 4b). However, in the exponential growth phase the breast cancer cell lines showed similar modes of spin probe motion as nonmalignant cell lines, which had approximately constant plasma membrane fluidity, irrespective of cell density or cell growth time (Figure 4c).

DISCUSSION

It is well-known that membrane fluidity is altered in tumor cells and increases with the proliferative activity of cells. Malignant cells are susceptible to external fluidity modulators, while normal cells maintain their specific membrane fluidity irrespective of the composition of the various chemical constituents in the external fluid. The homeostasis mechanism of membrane fluidity (homeoviscous adaptation) operates mostly via alterations in the degree of unsaturation of the membrane phospholipids and in the level of cholesterol in the membrane of normal cells.[2] In the recent models of a cell membrane and with recent experiments emphasis in the investigation of cell membranes is shifted from the characterization of membrane fluidity to the characterization of the domain structure of membranes. In the more recent views, the Singer−Nicolson mosaic model is still valid but only within domains where lipids can undergo free diffusion. A new paradigm of cell membranes treats the membrane as a compartmentalized, quasi two-dimensional, mosaic fluid with supramolecular structures that are dynamically generated and destroyed,[9] with the free lateral diffusion of proteins and lipids limited to the size of compartments (typically several ten to several hundred nanometers in radius), with infrequent intercompartment transitions.[10,11,25] It is therefore mandatory to study the domain structure of lipid membranes, to understand the physiology of cells.

Therefore, the aim of our study is not to confirm already established data about the differences in membrane fluidity of malignant and nonmalignant cells and to discuss how different membrane constituents, like cholesterol, proteins, and the unsaturation of lipids, influence membrane fluidity but to show that also the membrane domain structure of malignant cells changes with increasing cell density and the time of cell growth and to discuss the probable consequences of this membrane property. This is enabled now with the development of the computer simulation of the EPR spectra with the GHOST optimization procedure.[22] For this purpose we have chosen four different malignant cell lines of different origin (human breast cancer cells and human cervical adenocarcinoma) and two different nonmalignant cell lines from different origins, to see if the observations obtained are valid generally for different tumor cell lines. We confirmed previous experiments, which demonstrated cell density dependent alterations of the membrane fluidity of malignant cells,[2] which were not observed in contact-inhibited nonmalignant cells and extended these observations to the determination of the membrane domain structure. The EPR spectra of a lipophilic fatty acid spin probe showed an increase in membrane fluidity with an increasing cell density of cancer cells. Additionally, with the newly developed GHOST condensation procedure, by which it is possible to determine different modes of the spin probe motion that reflect the properties of their environment, a more detailed view of the heterogeneous cell membrane structure during cell growth and with increasing cell density was obtained. For malignant cells in the exponential growth phase more modes of the spin probe motion were observed as for the

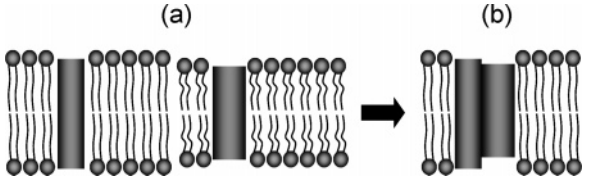

Figure 5. Membrane switch hypothesis. A schematic presentation of ligand cluster formation promoted by a disappearance of a membrane domain: (a) a part of a plasma membrane with two coexisting membrane domains and with membrane proteins separated each in its own membrane domain and (b) a part of a plasma membrane with only one remaining membrane domain into which both kinds of membrane proteins are clustered.

cells in the confluent phase (Figures 3 and 4). This is especially well expressed in MT1 cells, where five distinct membrane domains were detected. The number of these domains decreased to three in the plateau phase when the cell density was approximately twice as high as compared to the cell density in the exponential phase of growth (Figure 3). The two modes of spin probe motion, one characterized with order parameter $S \sim 0.3$ and a highly polar environment ($p_A \sim 1.05$), and the second with $S \sim 0.2$ and a nonpolar environment ($p_A \sim 0.85$), disappeared in the confluent phase. As already mentioned different modes of the spin probe motion reflect the properties of its surrounding and describe the properties of different domain types in the membrane or different positions of spin probes in a domain.

The lipid membrane could promote membrane protein clustering in two ways: by the disappearance of membrane domains and by the emergence of new domains with intermediate dynamic properties of membrane constituents of already existing domains. When the domain disappears, proteins residing in this domain must partition in another more suitable domain that is still present, where they can meet other proteins, originally residing in this domain (Figure 5). When a new domain appears, it might connect two previously present domains and in this way provide a bridge between two domains, providing a contact of membrane proteins, which were previously separated in their own domains.[26] Alterations in the membrane domain structure can originate in the different lipid composition of cell membranes, as it was observed for malignant cells.

Clustering of proteins and other membrane constituents may have a serious consequence/impact on physiological properties of cells. In nonmalignant cells similar patterns on the GHOST diagrams were observed as in malignant cells in the exponential phase, which do not change significantly with the time of cell growth or with cell density.

On the basis of our experiments we assume that the alteration of the membrane domain structure and the disappearance of membrane domains could act as a switch, promoting clustering of membrane constituents. A similar idea that percolating properties of membrane domains may serve as a potential trigger mechanism in the control of membrane physiology was already proposed.[27,28] Our results show that in malignant cells the membrane domain structure is much more sensitive to changes in the cell environment in comparison to that of nonmalignant cells and provide new information with respect to the previous findings concerning the differences in membrane fluidity of malignant and normal cells.[2] We speculate that in malignant cells, due to the disappearance of some membrane domains, clustering of membrane constituents, proteins, and other ligands can occur.

This might be important for cancer metastasis when a close adhesion of a cancer cell to the endothelial membrane is necessary as the first step in the metastatic cascade prior to tumor cell invasion into a tissue. Such an adhesion can be mediated by specific ligands expressed by tumor cells, which specifically bind to E-selectin, expressed on the endothelial surface.[29,30] Several studies demonstrated that the binding of a monovalent ligand to the corresponding receptor is too weak to obtain a sufficient attachment of the tumor cell at the endothelial surface, whereas a multivalent ligand system works much better.[31−34] Multivalent peptides and proteins with several binding sites provide such efficient binding systems.[35] We assume that one of the mechanisms promoting the tumor cell adhesion to the endothelial receptors could be the clustering of ligands in the tumor cell membrane. According to our assumption this ability should be enhanced when the fluidity of tumor cells is increased during cell growth and some domains disappear. The disappearance of a membrane domain type during cell growth might promote cluster formation of ligands by forcing the ligands previously located in separated membrane domains into the only remaining domain and trigger the formation of a multivalent binding site (Figure 5). This assumption is a matter of our further investigation.

Since our preliminary data in Figure 4 suggest that the membrane domain structure of contact inhibited V79 hamster fibroblasts and HEK-293 human embryonic kidney cells does not change substantially during cell growth or with increasing cell density, further studies are necessary to answer the question whether the membrane domain structure is involved in contact inhibition of cell growth. Successive B16 melanoma tumor cell lines might serve as a model for this study, because they have variable metastatic capability.[36]

CONCLUSION

We demonstrated that the cell growth−cell density related increase of plasma membrane fluidity of cancer cells is accompanied by the disappearance of some plasma membrane domains. On these grounds and because of the importance of ligand cluster formation during the different metabolic processes of cells, we propose a "membrane switch hypothesis", which takes into account that membrane protein cluster formation might be promoted by alterations in membrane domain organization.

ACKNOWLEDGMENT

This work was carried out with the financial support of the Ministry of High Education, Science and Technology of the Republic of Slovenia and in part by the German Ministry of Education and Research (BMBF).

REFERENCES AND NOTES

(1) Kim, Y. C.; Ntambi, J. M. Regulation of stearoyl-CoA desaturase genes: role in cellular metabolism and preadipocyte differentiation. *Biochem. Biophys. Res. Commun.* **1999**, *266*, 1−4.

(2) Shinitzky, M. Membrane fluidity in malignancy. Adversative and recuperative. *Biochim. Biophys. Acta* **1984**, *738*, 251−261.

(3) Taraboletti, G.; Perin, L.; Bottazzi, B.; Mantovani, A.; Giavazzi, R.; Salmona, M. Membrane fluidity affects tumor-cell motility, invasion and lung-colonizing potential. *Int. J. Cancer* **1989**, *44*, 707−713.

(4) van Blitterswijk, W. J.; Hilkmann, H.; Storme, G. A. Accumulation of an alkyl lysophospholipid in tumor cell membranes affects membrane fluidity and tumor cell invasion. *Lipids* **1987**, *22*, 820−823.
(5) Sok, M.; Sentjurc, M.; Schara, M. Membrane fluidity characteristics of human lung cancer. *Cancer Lett.* **1999**, *139*, 215−220.
(6) Sok, M.; Sentjurc, M.; Schara, M.; Stare, J.; Rott, T. Cell membrane fluidity and prognosis of lung cancer. *Ann. Thorac. Surg.* **2002**, *73*, 1567−1571.
(7) Rivnay, B.; Gorelik, E.; Segal, S.; Shinitzky, M. Plasma membrane microviscosity of Lewis lung carcinoma cells derived from local growth and pulmonary metastases. *Invasion Metastasis* **1981**, *1*, 99−110.
(8) Singer, S. J.; Nicolson, G. L. The fluid mosaic model of the structure of cell membranes. *Science* **1972**, *175*, 720−731.
(9) Vereb, G.; Szollosi, J.; Matko, J.; Nagy, P.; Farkas, T.; Vigh, L.; Matyus, L.; Waldmann, T. A.; Damjanovich, S. Dynamic, yet structured: The cell membrane three decades after the Singer-Nicolson model. *Proc. Natl. Acad. Sci. U.S.A.* **2003**, *100*, 8053−8058.
(10) Fujiwara, T.; Ritchie, K.; Murakoshi, H.; Jacobson, K.; Kusumi, A. Phospholipids undergo hop diffusion in compartmentalized cell membrane. *J. Cell Biol.* **2002**, *157*, 1071−1081.
(11) Murase, K.; Fujiwara, T.; Umemura, Y.; Suzuki, K.; Iino, R.; Yamashita, H.; Saito, M.; Murakoshi, H.; Ritchie, K.; Kusumi, A. Ultrafine membrane compartments for molecular diffusion as revealed by single molecule techniques. *Biophys. J.* **2004**, *86*, 4075−4093.
(12) Bearden, J. C. J. Quantitation of submicrogram quantities of protein by an improved protein-dye binding assay. *Biochim. Biophys. Acta* **1978**, *533*, 525−529.
(13) Budil, D. E.; Lee, S.; Saxena, S.; Freed, J. H. Nonlinear-Least-Squares Analysis of Slow-Motion EPR Spectra in One and Two Dimensions Using a Modified Levenberg−Marquardt Algorithm. *J. Magn. Reson. A* **1996**, *120*, 155.
(14) Robinson, B. T., H.; Beth, A. H.; Fajer, P.; Dalton, L. R. The phenomenon of magnetic resonance: Theoretical considerations. In *EPR and Advanced EPR Studies of Biological Systems*; Dalton, L. R., Ed.; CRC Press: Boca Raton, 1985; p 99.
(15) Schneider, D. J.; Freed, J. H. Calculating slow motional magnetic resonance spectra: a user's guide. In *Biological Magnetic Resonance: Spin Labeling Theory and Applications*; Berliner, L. J., Reuben, J., Ed.; Plenum Press: New York, 1989; p 76.
(16) Schindler, H. S., J. EPR spectra of spin labels in lipid bilayers. *J. Chem. Phys.* **1973**, *59*, 1841−1850.
(17) Strancar, J.; Sentjurc, M.; Schara, M. Fast and accurate characterization of biological membranes by EPR spectral simulations of nitroxides. *J. Magn. Reson.* **2000**, *142*, 254−265.
(18) Strancar, J.; Koklic, T.; Arsov, Z. Soft picture of lateral heterogeneity in biomembranes. *J. Membr. Biol.* **2003**, *196*, 135−146.
(19) Johnson, M. E.; Berk, D. A.; Blankschtein, D.; Golan, D. E.; Jain, R. K.; Langer, R. S. Lateral diffusion of small compounds in human stratum corneum and model lipid bilayer systems. *Biophys. J.* **1996**, *71*, 2656−2668.
(20) Trauble, H.; Sackmann, E. Studies of the crystalline-liquid crystalline phase transition of lipid model membranes. 3. Structure of a steroid-lecithin system below and above the lipid-phase transition. *J. Am. Chem. Soc.* **1972**, *94*, 4499−4510.
(21) Filipic, B.; Strancar, J. Tuning EPR spectral parameters with a genetic algorithm. *Applied Soft Computing* **2001**, *1*, 83.
(22) Strancar, J.; Koklic, T.; Arsov, Z.; Filipic, B.; Stopar, D.; Hemminga, M. A. Spin Label EPR−Based Characterization of Biosystem Complexity. *J. Chem. Inf. Model.* **2005**, *45*, 394−406.
(23) Swartz, H. M.; Sentjurc, M.; Morse, P. D., 2nd. Cellular metabolism of water-soluble nitroxides: effect on rate of reduction of cell/nitroxide ratio, oxygen concentrations and permeability of nitroxides. *Biochim. Biophys. Acta* **1986**, *888*, 82−90.
(24) Ueda, A.; Nagase, S.; Yokoyama, H.; Tada, M.; Noda, H.; Ohya, H.; Kamada, H.; Hirayama, A.; Koyama, A. Importance of renal mitochondria in the reduction of TEMPOL, a nitroxide radical. *Mol. Cell Biochem.* **2003**, *244*, 119−124.
(25) Kusumi, A.; Ike, H.; Nakada, C.; Murase, K.; Fujiwara, T. Single-molecule tracking of membrane molecules: plasma membrane compartmentalization and dynamic assembly of raft-philic signaling molecules. *Semin. Immunol.* **2005**, *17*, 3−21.
(26) Kramarič, P.; Pavlica, Z.; Koklič, T.; Nemec, A.; Kožuh Eržen, N.; Šentjurc, M. Membrane switch hypothesis. 2. domain structure of phagocytes in horses with recurrent airway obstruction. *J. Chem. Inf. Model.* **2005**, 45, 1708−1715.
(27) Vaz, W. L. Diffusion and chemical reactions in phase-separated membranes. *Biophys. Chem.* **1994**, *50*, 139−145.
(28) Vaz, W. L. Percolation properties of two-component, two-phase phospholipid bilayers. *Mol. Membr. Biol.* **1995**, *12*, 39−43.
(29) Engers, R.; Gabbert, H. E. Mechanisms of tumor metastasis: cell biological aspects and clinical implications. *J. Cancer Res. Clin. Oncol.* **2000**, *126*, 682−692.
(30) Kannagi, R. Carbohydrate-mediated cell adhesion involved in hematogenous metastasis of cancer. *Glycoconjugate J.* **1997**, *14*, 577−584.
(31) Gordon, E. J.; Gestwicki, J. E.; Strong, L. E.; Kiessling, L. L. Synthesis of end-labeled multivalent ligands for exploring cell-surface-receptor−ligand interactions. *Chem. Biol.* **2000**, *7*, 9−16.
(32) Stahn, R.; Zeisig, R. Cell adhesion inhibition by glycoliposomes: effects of vesicle diameter and ligand density. *Tumor Biol.* **2000**, *21*, 176−186.
(33) Vogel, J.; Bendas, G.; Bakowsky, U.; Hummel, G.; Schmidt, R. R.; Kettmann, U.; Rothe, U. The role of glycolipids in mediating cell adhesion: a flow chamber study. *Biochim. Biophys. Acta* **1998**, *1372*, 205−215.
(34) Zeisig, R.; Stahn, R.; Wenzel, K.; Behrens, D.; Fichtner, I. Effect of sialyl Lewis X-glycoliposomes on the inhibition of E-selectin-mediated tumour cell adhesion in vitro. *Biochim. Biophys. Acta* **2004**, *1660*, 31−40.
(35) Stahn, R.; Schafer, H.; Kernchen, F.; Schreiber, J. Multivalent sialyl Lewis x ligands of definite structures as inhibitors of E-selectin mediated cell adhesion. *Glycobiology* **1998**, *8*, 311−319.
(36) Fidler, I. J. Biological behavior of malignant melanoma cells correlated to their survival in vivo. *Cancer Res.* **1975**, *35*, 218−224.

CI050186R